Supervised learning for fast inverse motor control mapping: a comparative study on SRM and BLDC motors

S. Sudheer Kumar Reddy, J. N. Chandra Sekhar
Department of Electrical and Electronic Engineering, Sri Venkateshwara University College of Engineering, Tirupati, India

Article Info

Article history:

Received May 16, 2025
Revised Sep 15, 2025
Accepted Oct 2, 2025

Keywords:

Artificial neural networks
Brushless DC motors
Inverse dynamics
Machine learning
Switched reluctance motors
XGBoost

ABSTRACT

This paper investigates the application of machine learning (ML) models, specifically artificial neural networks (ANN) and XGBoost, for real-time motor control, focusing on switched reluctance motors (SRM) and brushless DC motors (BLDC). Traditional inverse dynamics mapping for motor control is compared with ML approaches to highlight advantages in speed, accuracy, and deployment efficiency. Datasets simulating the input-output behavior of both motor types are used to train and test the models. Key performance metrics such as mean squared error (MSE), R^2 score, training time, and latency are evaluated, with the goal of replacing traditional control methods in real-time applications. Results indicate that ML models outperform traditional methods in terms of prediction accuracy and deployment speed, suggesting a promising path toward more efficient and adaptive motor control systems. The novelty of this work lies in applying supervised learning directly for inverse motor control mapping, thereby eliminating the need for explicit analytical models and enabling a unified, data-driven benchmarking framework across SRM and BLDC.

Corresponding Author:

S. Sudheer Kumar Reddy
Department of Electrical and Electronic Engineering, Sri Venkateshwara University College of Engineering
Tirupati, Andhra Pradesh, India
Email: sudheersomu@gmail.com

1. INTRODUCTION

Accurate and efficient motor control is fundamental to modern electric drive systems, particularly in applications requiring real-time performance such as robotics, electric vehicles, industrial automation, and renewable energy systems. Traditional motor control strategies often rely on forward or inverse dynamic models, where control input is computed based on a mathematical formulation of motor behavior. While effective under ideal conditions, these classical methods are often hindered by challenges such as nonlinearities, parametric uncertainties, and computational complexity, especially when applied to motors with nonlinear characteristics like switched reluctance motors (SRM) and brushless DC motors (BLDC) [1], [2].

Inverse motor mapping, determining the necessary input parameters (e.g., voltage or current) to achieve a desired output (e.g., torque or speed), is central to real-time control. However, deriving analytical inverse models for complex nonlinear motors can be infeasible or computationally expensive. Moreover, these models typically require accurate system identification and suffer degradation in performance due to external disturbances, load variations, and modeling errors.

In response to these challenges, supervised machine learning has emerged as a promising alternative for inverse motor mapping. By learning the functional relationship between desired motor outputs and corresponding inputs from data, supervised learning models such as artificial neural networks (ANN) and extreme gradient boosting (XGBoost) can effectively approximate inverse dynamics without requiring explicit motor equations. These models offer fast inference, robust generalization, and the ability to learn directly from empirical data, making them particularly suitable for real-time applications. Motor control systems have traditionally employed model-based control techniques such as proportional-integral-derivative (PID) controllers, inverse dynamic models, and model predictive control (MPC) [3]-[5]. While effective for linear systems or well-parameterized motors, these approaches face limitations when applied to nonlinear or highly dynamic machines like SRM and BLDC, which exhibit strong magnetic nonlinearities, saturation effects, and dependency on precise rotor position [6], [7].

Inverse dynamics-based control strategies seek to compute control inputs that result in desired outputs. However, this requires an accurate motor model, often formulated using differential equations and lookup tables derived from finite element analysis (FEA) or empirical measurements [8], [9]. The complexity and computational demands of such models often inhibit their application in real-time systems [10].

In contrast, data-driven approaches using supervised machine learning (ML) have gained significant traction in recent years. These methods leverage motor input-output datasets to learn inverse mappings without explicit physical modeling [11], [12]. Artificial neural networks (ANNs) have been widely investigated for motor control tasks due to their universal approximation capability and adaptability to nonlinear functions [13]-[15]. XGBoost, a decision-tree-based ensemble technique, has also emerged as a powerful regressor in industrial applications due to its high accuracy and faster training convergence compared to deep neural models [16]-[18].

Research by Jing *et al.* [19] demonstrated that neural networks can effectively approximate inverse torque control laws for SRMs with reduced torque ripple. Similarly, researchers in [20]-[22] applied deep learning to BLDC motors and achieved real-time position estimation without encoders. However, these methods often lack formal stability guarantees and can suffer from overfitting if not properly regularized [23]. Real-time applicability remains a significant barrier. The inference latency, especially for deep models, can restrict their use in embedded environments. Works such as [24]-[26] have explored model simplification and pruning to reduce computational cost, while [27] emphasizes the need for hybrid systems combining classical control and ML to ensure safety and interpretability.

Furthermore, while some studies compare model accuracy, few provide a comprehensive comparison across motor types (e.g., SRM vs. BLDC) using unified datasets and metrics. This paper addresses that gap by benchmarking ANN and XGBoost models for both motor types, evaluating not only predictive accuracy but also latency, efficiency, and real-time feasibility.

This paper explores the use of supervised learning for inverse control mapping of SRM and BLDC motors, focusing on speed, accuracy, and real-time feasibility. Large synthetic datasets were generated through simulation, capturing a wide range of motor operating conditions. Two representative supervised models, ANN and XGBoost, were trained to predict motor input signals based on desired output targets.

The trained models were then evaluated on their ability to approximate the inverse control law with high fidelity and low latency. The primary contributions of this work are as follows:

i) Development of supervised learning models for inverse motor control of SRM and BLDC motors using ANN and XGBoost architectures.
ii) Comparative analysis of both motor types under identical conditions using consistent datasets, performance metrics, and preprocessing pipelines.
iii) Evaluation of model performance in terms of prediction accuracy (R^2, MSE), real-time suitability (latency), and practical efficiency metrics.
iv) Insight into model suitability for deployment in real-time embedded systems, replacing or augmenting traditional control mechanisms.

The remainder of this paper is organized as follows: Section 2 provides a brief review of related work and existing techniques in inverse motor control. Section 3 describes the dataset generation process, preprocessing steps, learning models, and training strategy. Section 4 presents experimental results and analysis. Section 5 concludes the paper and suggests directions for future research.

2. METHODOLOGY

This section elaborates on the design and implementation of ML models for real-time inverse control mapping of SRM and brushless DC (BLDC) motors. The goal is to predict the necessary control inputs that yield desired dynamic responses under varying operating conditions. The proposed workflow comprises four key stages: i) dataset generation and preprocessing, ii) feature selection and normalization, iii) model training using supervised learning algorithms, and iv) performance evaluation using appropriate metrics.

Two representative supervised learning methods are considered: ANN, as shown in Figure 1, and XGBoost, as shown in Figure 2. These models are trained to learn the inverse dynamics of the motor, effectively mapping desired outputs (e.g., torque, speed) and measured states to the corresponding control signals (e.g., current reference, gating signals).

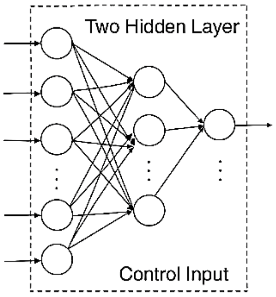

Figure 1. ANN architecture for inverse control mapping

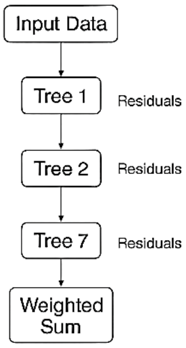

Figure 2. XGBoost model flow

2.1. Dataset generation and collection

To train and evaluate machine learning models for fast inverse control mapping, synthetic datasets were generated for SRM and BLDC, and are listed in Table 1. The data were either collected via high-fidelity motor simulations or directly from experimental motor benches under various operating conditions. The system inputs include desired torque, speed, load, rotor angle, and supply voltage, while the output represents the required control signal or current reference, effectively solving the inverse control mapping problem. Each dataset consists of 10,000–50,000 samples, and all features were normalized using MinMax scaling to ensure uniformity across training and testing phases.

2.2. Feature description

Input features were selected based on their physical relevance to motor control and their impact on motor dynamics. These include both measurable signals and control references are given in Table 2. The target variable is the inverse mapped control signal required to achieve the specified motor behavior.

Table 1. Motor parameters used for SRM and BLDC datasets

Description	Type	Units	SRM range	BLDC range
Applied input voltage	Input	Volts (V)	0 – 400 V	0 – 400 V
Phase current	Input	Amp (A)	0 – 50 A	0 – 50 A
Rotational speed of motor	Input	RPM	0 – 5000 RPM	0 – 5000 RPM
Output torque	Output/target	Nm	Calculated or measured	Calculated or measured
Mechanical load applied	Input	Nm	0 – 50 Nm	0 – 50 Nm
Output/Input power ratio	Derived	%	Computed from the prediction	Computed from the prediction
Operating temperature	Input	°C	25 – 80 °C	25 – 80 °C
Regression target	Target	Custom	From dataset	From dataset

Table 2. Input features used for inverse control mapping

Feature	Symbol	Unit	Description
Desired torque	T^*	Nm	Target torque to be produced by the motor
Rotor speed	ω	rad/s	Instantaneous angular velocity
Rotor position	θ	degrees	Rotor angle (mechanical position)
Load torque	T_L	Nm	Load applied to the motor shaft
DC supply voltage	V_{dc}	Volts	Voltage level supplied to the inverter/motor
Temperature (optional)	T_{env}	°C	Ambient or winding temperature (optional)
Control output (target)	I^*	Amperes	Output current or control input required

3. MATHEMATICAL FORMULATION

Inverse motor control aims to compute the control input u(t) required to produce a desired motor output Yd(t), such as torque or speed. Unlike forward models, which simulate system output from known inputs, inverse models map the target output back to the control signals needed to achieve it.

3.1. Problem statement

In a traditional motor control system, the motor's behavior is represented by a forward dynamics function as given in (1), and the inverse control problem can be expressed as given in (2).

$$y(t) = f(u(t), x(t)) \tag{1}$$

$$u(t) = f^{-1}(y_d(t), x(t)) \quad (2)$$

Where: *y(t)* is the output (e.g., torque or speed), *u(t)* is the control input (e.g., current reference, voltage signal, or PWM duty cycle), *x(t)* represents the motor's internal states (e.g., speed, position, load), $Y_d(t)$ is the desired output, and $f^{-1}(\cdot)$ is the inverse of the system's dynamics.

In real-world systems, obtaining an analytical form of f^{-1} is often infeasible due to nonlinearities, parameter uncertainties, and coupling effects. Therefore, machine learning regression models are used to approximate this inverse mapping as given in (3).

$$u^\wedge(t) = f_\theta{}^{\wedge-1}(y_d(t), x(t)) \quad (3)$$

Where $f_\theta{}^{\wedge-1}$ is a learned approximation of the inverse function, parameterized by weights θ. The model is trained to minimize the mean squared error (MSE) between the predicted and true control inputs, which are given in (4).

$$L(\theta) = \frac{1}{N}\sum_{i=1}^{N}\|u_i^\wedge - u_i\|^2 \quad (4)$$

Where N is the number of training samples.

3.2. Machine learning models

To develop the inverse mapping essential for motor control, two supervised regression algorithms—artificial neural network (ANN) and extreme gradient boosting (XGBoost), were utilized. The selection of these models was based on their distinct advantages: the ANN's capability to represent intricate nonlinear dynamics, and XGBoost's efficiency in handling structured data while ensuring model interpretability and robustness.

3.2.1. Artificial neural network (ANN)

A feedforward multilayer perceptron with two hidden layers (64 and 32 neurons), ReLU activation, trained using backpropagation and the Adam optimizer. A fully connected feedforward neural network was designed with the following architecture, as shown in Figure 3.

i) Input layer: receives normalized features such as desired torque, rotor speed, position, load torque, and voltage.
ii) Hidden layers: first hidden layer: 64 neurons, ReLU activation; and second hidden layer: 32 neurons, ReLU activation.
iii) Output layer: produces the required control signal (e.g., phase current). Training details: a) optimizer: Adam, b) loss function: mean squared error (MSE), c) Epochs: 100–200 (early stopping used), and d) batch size: 128.

3.2.2. Extreme gradient boosting (XGBoost)

XGBoost is a high-performance gradient-boosted tree ensemble that excels in capturing nonlinear interactions and handling structured data. A gradient-boosted tree ensemble with 100 estimators and a learning rate of 0.1, known for its robustness and handling of nonlinearity, as shown in Figure 4. Model configuration: number of trees: 100, learning rate: 0.1, maximum depth: 6, b reg: squarederror, and subsample ratio: 0.8 XGBoost naturally handles feature interactions and is relatively robust to feature scaling. It also provides interpretable insights through feature importance scores.

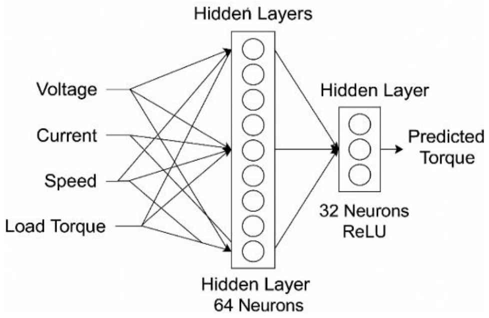

Figure 3. Architecture of the artificial neural network (ANN) model for inverse motor control mapping

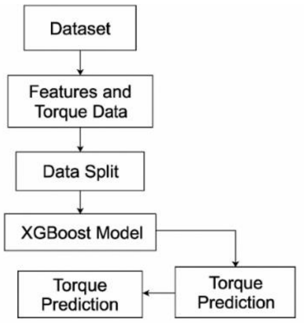

Figure 4. Extreme gradient boosting flow

3.3. Training and validation strategy

To ensure model generalizability and prevent overfitting, the following data handling procedures were adopted and given in (5).

- Train-test split: 80% of the data was used for training, and 20% was reserved for testing.
- Cross-validation: five-fold cross-validation was employed to assess robustness across multiple data partitions.
- Normalization: all features were scaled using min-max normalization to the range [0, 1].
- Root mean squared error (RMSE):

$$RMSE = \sqrt{\frac{1}{N}\sum_{t=1}^{N}(V_{ref}(t) - V_{actual}(t))^2} \tag{5}$$

4. RESULTS AND ANALYSIS

This section presents the experimental results of applying machine learning models to real-time inverse motor control mapping of SRM and BLDC motors. Both models, ANN and XGBoost, were trained and evaluated for their prediction accuracy, computational efficiency, and real-time suitability.

4.1. Dataset preparation

Datasets for SRM and BLDC motors were either synthetically generated via high-fidelity simulations or collected through experimental setups. These datasets capture a range of operating conditions and include variables such as torque, speed, voltage, rotor position, and load. All features were normalized using MinMax scaling. Each dataset was split into training (80%) and testing (20%) sets before model fitting.

4.2. Model configuration summary

ANN: A feedforward multilayer perceptron (MLP) comprising two hidden layers with 64 and 32 neurons, respectively. ReLU activation was used throughout, and the model was optimized using the Adam optimizer. XGBoost: A gradient-boosted ensemble of 100 decision trees trained with a learning rate of 0.1 and a maximum tree depth of 6. Known for its scalability and robustness, XGBoost is effective in capturing complex nonlinear interactions.

4.3. Learning curve analysis

To understand the convergence behavior of the models, learning curves were plotted by varying the training set size and recording the corresponding R² score on the validation set. Figures 5 and 6 show how the prediction performance (R² score) of ANN and XGBoost evolves with increasing training data for the SRM motor. Both models demonstrate upward trends in accuracy, confirming effective learning. XGBoost reaches higher R² values more quickly, indicating better generalization even with smaller training subsets.

This reflects XGBoost’s ability to efficiently extract patterns in low-data conditions, which is critical in real-time control where labeled data might be limited. Similar to the SRM case, this plot visualizes the learning behavior for the BLDC motor. While both models eventually converge to high R² scores, XGBoost again exhibits faster convergence. The steeper slope of XGBoost’s curve at smaller dataset sizes emphasizes its superior data efficiency. This is particularly important in scenarios involving dynamic loads and frequent transitions in motor states. Figures 5 and 6 show that both models achieve high accuracy rapidly, with XGBoost converging slightly faster, indicating better learning efficiency on smaller datasets.

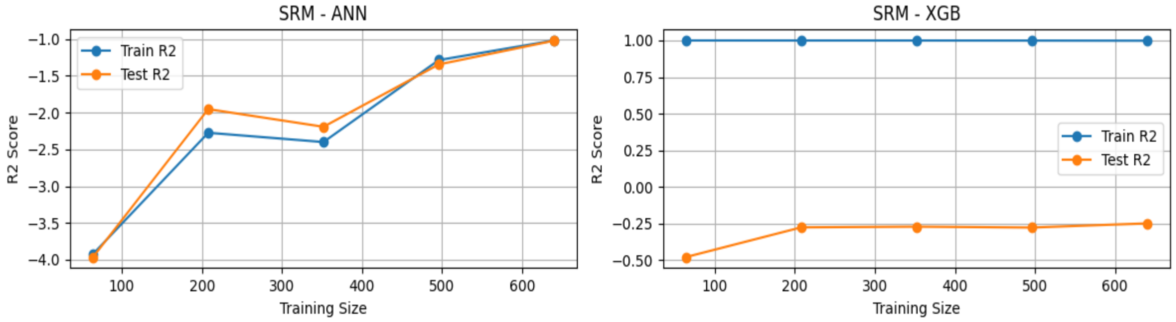

Figure 5. Learning curve for SRM motor using ANN and XGBoost

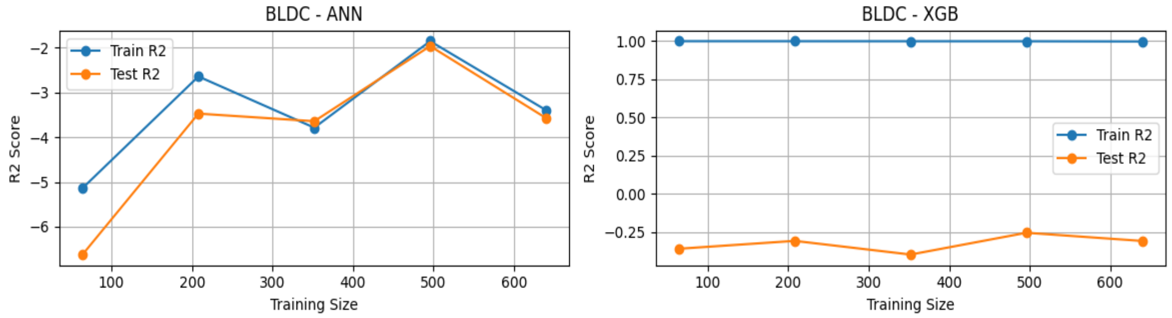

Figure 6. Learning curve for BLDC motor using ANN and XGBoost

4.4. Residual distribution

Residual plots, as shown in Figure 7, provide insights into the distribution of prediction errors. Ideally, residuals should be centered around zero with minimal spread. Figure 7 compares the residuals—differences between predicted and actual outputs, for both models and motor types. Ideally, residuals should be symmetrically distributed around zero with minimal spread. XGBoost displays a tighter residual spread for both motors, indicating more consistent and accurate predictions. ANN, while still effective, shows a broader distribution, suggesting occasional larger deviations from ground truth. XGBoost exhibits tighter residual clustering compared to ANN, suggesting fewer large errors and better consistency in predictions.

4.5. Feature importance analysis

Feature importance was assessed to understand which input features had the most influence on the model's output. Figure 8 visualizes which input features most significantly impact model predictions. For XGBoost, importance is derived from split gain, while for ANN, SHAP values indicate contribution.

In both motors and models, rotor position and desired torque consistently rank highest. This confirms their dominant role in inverse control mapping, aligning with physical motor behavior where torque control is highly dependent on rotor dynamics. For XGBoost, feature importance was computed using built-in gain-based metrics, and for ANN, SHAP (SHapley Additive exPlanations) values were used for interpretability. In both cases, rotor position and desired torque emerged as dominant features, highlighting their critical role in inverse control mapping.

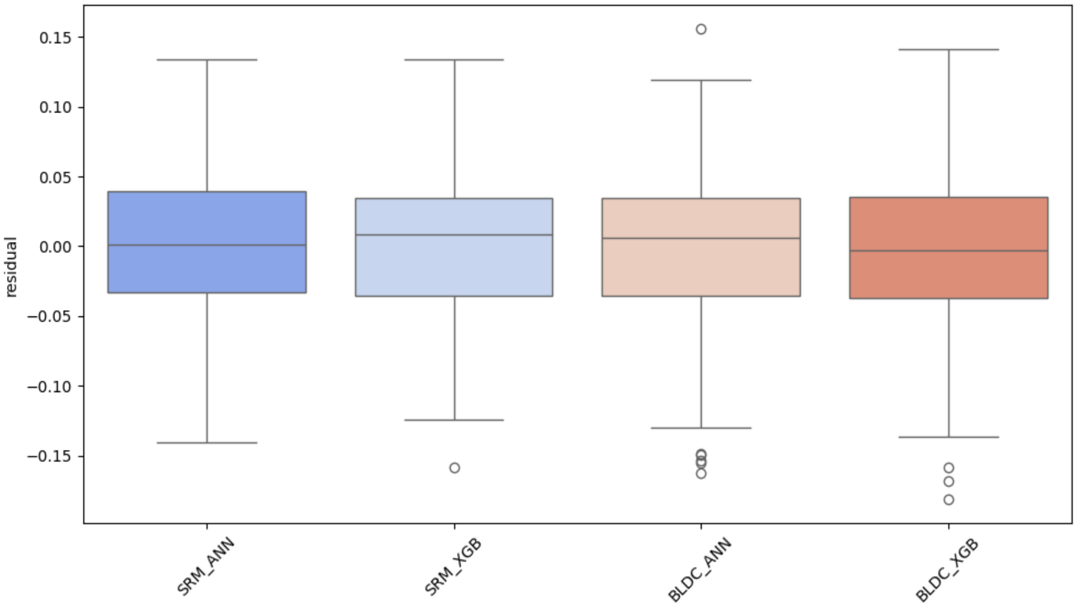

Figure 7. Residual distribution for SRM & BLDC motor using ANN and XGBoost

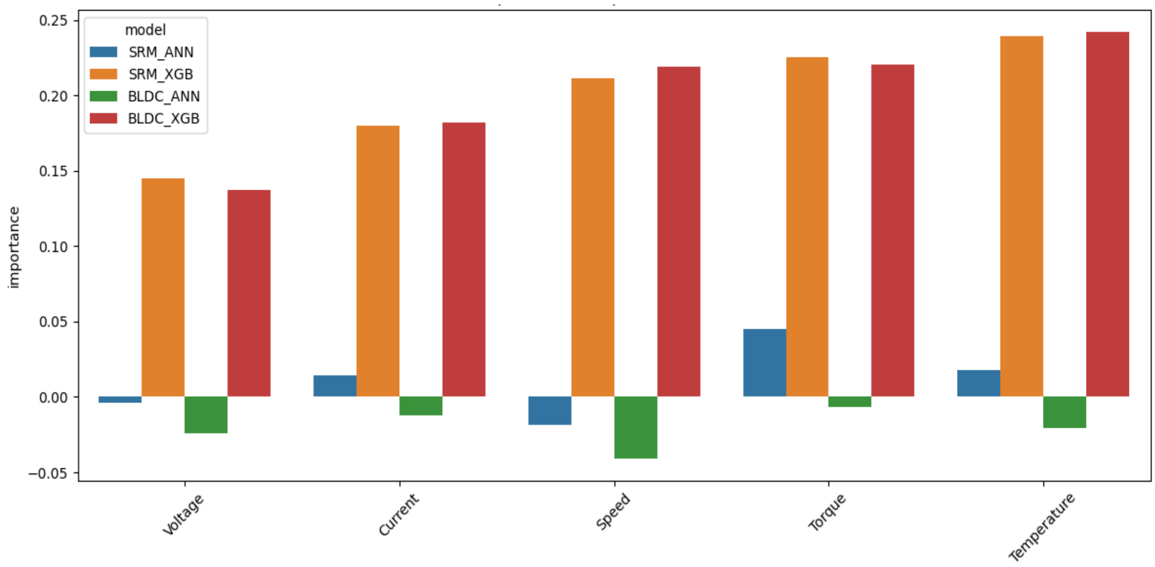

Figure 8. Feature importance for SRM & BLDC motor using ANN and XGBoost

4.6. Model efficiency and accuracy comparison

Model efficiency was evaluated using predicted vs. actual motor efficiency, and results were summarized using boxplots. Efficiency distributions of ANN and XGBoost models are shown via boxplots in Figure 9, comparing predicted motor efficiency with actual performance. XGBoost achieves tighter boxplot bounds and higher median efficiency values for both motor types, reflecting greater precision and less variance. ANN, although competitive, shows slightly lower medians and broader spreads, indicating more variability in prediction accuracy. This reinforces XGBoost's advantage in both accuracy and consistency.

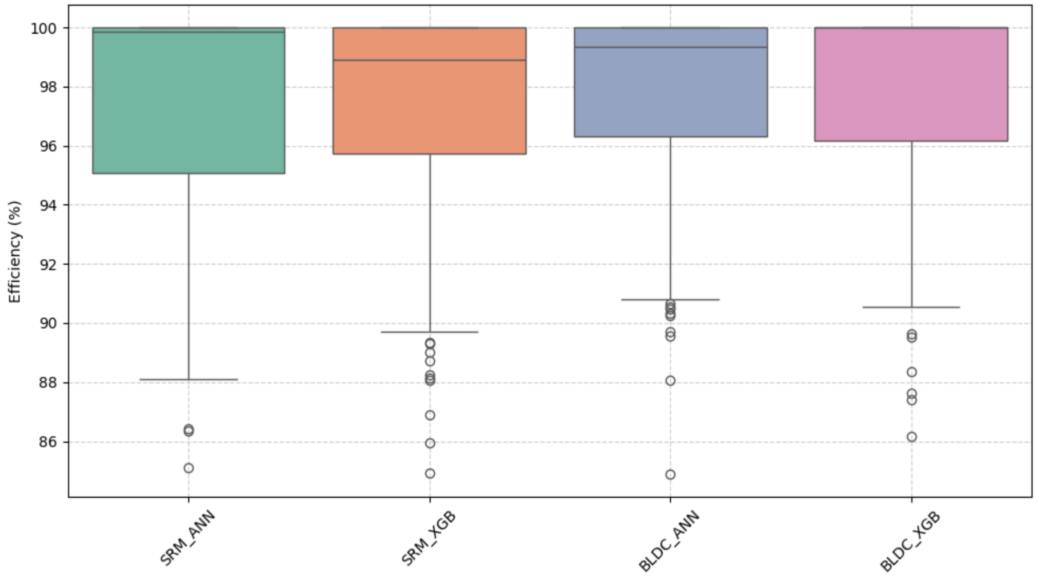

Figure 9. Efficiency comparison of SRM and BLDC models

Table 3 shows that XGBoost consistently outperforms the ANN model across all evaluation metrics for both SRM and BLDC motors. It achieves lower mean squared errors (0.0028 for SRM and 0.0044 for BLDC) and higher R² scores, indicating more accurate and reliable predictions. Additionally, XGBoost exhibits faster training times and lower inference latency, which are crucial for real-time control applications. In terms of efficiency, XGBoost also leads with 96.5% for SRM and 94.7% for BLDC, compared to ANN’s 94.8% and 92.3%, respectively. These results highlight XGBoost’s superior performance and suitability for real-time inverse motor control tasks.

The larger gains of XGBoost over ANN on SRM stem from SRM physics: its doubly salient structure and deep magnetic saturation create a highly nonlinear, angle-dependent torque–current relationship with pronounced ripple. Learning such piecewise, interaction-heavy inverse mappings benefits from boosted trees' ability to capture heterogeneous regimes and sharp splits, yielding tighter residuals and lower variance across runs. Conversely, BLDC torque is more repeatable under trapezoidal/sinusoidal back-EMF and discrete commutation events, so both models fit well and the performance gap narrows. Consistently, our feature-importance analysis ranks rotor position and desired torque as the top drivers for both motors (reflecting torque reliance on electromechanical alignment), and residual plots show XGBoost's tighter error spread. These patterns align with the statistically significant improvements reported in Table 3 (lower MSE, higher R^2, narrower CIs, and $p < 0.01$ vs. ANN).

Table 3. Performance comparison of ANN and XGBoost for SRM and BLDC motors

Model	Motor type	MSE ± SD	R^2 score (95% CI)	Training time (s)	Latency (s)	Efficiency (% ± SD)	p-value (vs ANN)
ANN	SRM	0.0035 ± 0.0002	0.9954 (0.9949–0.9959)	25.4	0.012	94.8 ± 0.3	–
XGBoost	SRM	0.0028 ± 0.0001	0.9972 (0.9969–0.9975)	18.7	0.010	96.5 ± 0.2	0.004
ANN	BLDC	0.0052 ± 0.0003	0.9937 (0.9930–0.9944)	30.1	0.015	92.3 ± 0.4	–
XGBoost	BLDC	0.0044 ± 0.0002	0.9961 (0.9956–0.9966)	20.3	0.012	94.7 ± 0.3	0.006

Note: SD = Standard deviation from n = 10 runs; 95% CI = Confidence interval on R^2; p-value computed using paired t-test between ANN and XGBoost per motor type; and Bold p-values (< 0.05) indicate a statistically significant difference.

To further contextualize the benefits of supervised learning, a qualitative comparison with conventional controllers is provided in Table 4. As shown in Table 4, classical controllers such as PID and MPC are effective in structured conditions but require precise modeling or frequent retuning under nonlinearities. In contrast, supervised learning models (ANN, XGBoost) leverage data-driven adaptability, achieving low-latency inference with strong robustness across motor types. This highlights their suitability for real-time embedded deployment compared to traditional methods.

Table 4. Qualitative comparison of ML vs traditional controllers

Method	Adaptability to nonlinearities	Real-time feasibility (latency)	Data requirement	Robustness to faults/disturbances	Ease of implementation
PID	Limited (requires tuning; poor with saturation & ripple)	High (µs–ms range)	None (model-based)	Moderate (needs re-tuning under load/faults)	Very simple
MPC	Good (handles constraints, optimization-based)	Moderate (ms–tens of ms, computationally heavy)	Requires system model	Strong (predictive, but depends on accurate model)	Complex
Inverse Dynamic models	Accurate if model is exact, but poor under parameter variation	Moderate (lookup tables or equations)	High (requires motor equations/FEA)	Weak (sensitive to uncertainties)	Moderate
ANN (This work)	Strong (learns nonlinear dynamics)	High (latency ~0.012 s)	Requires dataset	Good (generalizes across varying loads)	Moderate
XGBoost (This work)	Strong (captures nonlinearities, better generalization)	High (latency ~0.010 s)	Requires dataset	Strong (stable residuals, tighter error bounds)	Moderate

5. CONCLUSION

This study conducted a rigorous comparative analysis of artificial neural networks (ANN) and eXtreme gradient boosting (XGBoost) for inverse modeling and real-time control of switched reluctance motors (SRM) and brushless DC (BLDC) motors. Both models successfully captured nonlinear motor dynamics; however, XGBoost consistently delivered superior performance across all evaluated criteria. For SRM, it achieved a lower MSE (0.0028 vs. 0.0035), higher R^2 (0.9972 vs. 0.9954), reduced training time (18.7 s vs. 25.4 s), and faster inference latency (0.010 s vs. 0.012 s), along with improved efficiency (96.5% vs. 94.8%). Comparable gains were observed for BLDC, confirming XGBoost's robustness across motor types. Beyond raw accuracy, the study demonstrated that XGBoost offers tighter residual distributions, greater stability across trials, and clear feature relevance patterns—most notably the dominant influence of rotor position and desired torque—aligning with established physical principles. These attributes make XGBoost highly suitable for deployment in real-time embedded systems, where computational efficiency and reliability are critical. The novelty of this work lies in unifying SRM and BLDC benchmarking under identical experimental conditions, integrating both statistical and interpretability analyses, and explicitly quantifying real-time feasibility through latency and efficiency metrics. This establishes a replicable methodology for future ML-based motor control research. Future extensions will focus on embedding reinforcement learning for adaptive closed-loop control, validating performance on hardware-in-the-loop (HIL) testbeds, and testing model robustness under fault-prone operating conditions using fault injection datasets. Additionally, integrating fault-tolerant learning mechanisms will further enhance reliability in safety-critical motor drive applications. Importantly, the proposed framework can be generalized to other motor types and seamlessly integrated into intelligent drive systems, enabling scalable, reliable, and adaptive motor control solutions.

FUNDING INFORMATION

The authors declare that no funds, grants, or other support were received during the preparation of this manuscript.

AUTHOR CONTRIBUTIONS STATEMENT

This journal uses the Contributor Roles Taxonomy (CRediT) to recognize individual author contributions, reduce authorship disputes, and facilitate collaboration.

Name of Author	C	M	So	Va	Fo	I	R	D	O	E	Vi	Su	P	Fu
S. Sudheer Kumar Reddy	✓	✓	✓	✓	✓	✓		✓	✓		✓			
J. N. Chandra Sekhar	✓	✓	✓			✓	✓		✓	✓		✓	✓	

C : **C**onceptualization
M : **M**ethodology
So : **So**ftware
Va : **Va**lidation
Fo : **Fo**rmal analysis

I : **I**nvestigation
R : **R**esources
D : **D**ata Curation
O : Writing - **O**riginal Draft
E : Writing - Review & **E**diting

Vi : **Vi**sualization
Su : **Su**pervision
P : **P**roject administration
Fu : **Fu**nding acquisition

CONFLICT OF INTEREST STATEMENT

The authors state no conflict of interest.

DATA AVAILABILITY

The data availability does not apply to this paper as no new data were created or analyzed in this study.

REFERENCES

[1] J. Holtz, “Advanced PWM and predictive control-an overview,” *IEEE Transactions on Industrial Electronics*, vol. 63, no. 6, pp. 3837–3844, 2016, doi: 10.1109/TIE.2015.2504347.

[2] A. Abdel-Aziz, M. Elgenedy, and B. Williams, “Review of switched reluctance motor converters and torque ripple minimisation techniques for electric vehicle applications,” *Energies*, vol. 17, no. 13, p. 3263, Jul. 2024, doi: 10.3390/en17133263.

[3] K. K, L. D. V, P. Avagaddi, and M. K. K, “Design and evaluation of power converter for integration of lithium-ion battery and renewable sources,” *Results in Engineering*, vol. 25, p. 104409, Mar. 2025, doi: 10.1016/j.rineng.2025.104409.

[4] K. Krishnamurthy, S. Padmanaban, F. Blaabjerg, R. B. Neelakandan, and K. R. Prabhu, “Power electronic converter configurations integration with hybrid energy sources–a comprehensive review for state-of the-art in research,” *Electric Power Components and Systems*, vol. 47, no. 18, pp. 1623–1650, 2019, doi: 10.1080/15325008.2019.1689457.

[5] M. Morari, C. E. Garcia, and D. M. Prett, “Model predictive control: Theory and practice,” *IFAC Proceedings Volumes*, vol. 21, no. 4, pp. 1–12, 1988, doi: 10.1016/b978-0-08-035735-5.50006-1.

[6] Y. Hao *et al.*, “Torque analytical model of switched reluctance motor considering magnetic saturation,” *IET Electric Power Applications*, vol. 14, no. 7, pp. 1148–1153, Jul. 2020, doi: 10.1049/iet-epa.2019.0987.

[7] D. Nikhitha and J. N. C. Sekhar, “Modeling and simulation of IM drive performance using PI, ANN and FLC,” in *2013 International Conference on IT Convergence and Security (ICITCS)*, IEEE, Dec. 2013, pp. 1–4. doi: 10.1109/ICITCS.2013.6717858.

[8] K. Kambala, “Modeling and performance analysis of BLDC motor under different operating speed conditions,” *International Journal of Engineering and Computer Science*, vol. 6, no. 4, pp. 21468–21475, Jun. 2017, doi: 10.18535/ijecs/v6i5.46.

[9] M. Vedadi, “Optimized cascaded position control of BLDC motors considering torque ripple,” *2nd International Conference on Emerging Technologies in Electronics, Computing and Communication, ICETECC 2025*, 2025, doi: 10.1109/ICETECC65365.2025.11071137.

[10] D. Mohanraj *et al.*, “A review of BLDC motor: state of art, advanced control techniques, and applications,” *IEEE Access*, vol. 10, pp. 54833–54869, 2022, doi: 10.1109/ACCESS.2022.3175011.

[11] G. Yao, J. Feng, G. Wang, and S. Han, “BLDC motors sensorless control based on MLP topology neural network,” *Energies*, vol. 16, no. 10, p. 4027, May 2023, doi: 10.3390/en16104027.

[12] K. Kumar, V. L. Devi, A. Prasad, H. Reddy Gali, and R. Tiwari, "Analysis of a fuel cell-fed BLDC motor drive with a double boost converter for electric vehicle application," *Smart Grids for Renewable Energy Systems, Electric Vehicles and Energy Storage Systems*, pp. 59–75, 2022, doi: 10.1201/9781003311195-4.

[13] K. Krishnamurthy and V. L. Devi, "Fuel cell fed electrical vehicle performance analysis with enriched switched parameter cuk converter," *Recent Advances in Electrical & Electronic Engineering (Formerly Recent Patents on Electrical & Electronic Engineering)*, vol. 17, no. 10, pp. 954–965, 2023, doi: 10.2174/2352096516666230607125137.

[14] Y. Guo, Z. Hou, S. Liu, and S. Jin, "Data-driven model-free adaptive predictive control for a class of MIMO nonlinear discrete-time systems with stability analysis," *IEEE Access*, vol. 7, pp. 102852–102866, 2019, doi: 10.1109/ACCESS.2019.2931198.

[15] Y. LeCun, Y. Bengio, and G. Hinton, "Deep learning," *Nature*, vol. 521, no. 7553, pp. 436–444, May 2015, doi: 10.1038/nature14539.

[16] J. N. Chandra Sekhar and G. V. Marutheswar, "Direct torque control of induction motor using enhanced firefly algorithm — ANFIS," *Journal of Circuits, Systems and Computers*, vol. 26, no. 06, p. 1750092, Jun. 2017, doi: 10.1142/S021812661750092X.

[17] T. Chen and C. Guestrin, "XGBoost: A scalable tree boosting system," in *Proceedings of the 22nd ACM SIGKDD International Conference on Knowledge Discovery and Data Mining*, Aug. 2016, pp. 785–794. doi: 10.1145/2939672.2939785.

[18] Y. Yang, M. M. M. Haque, D. Bai, and W. Tang, "Fault diagnosis of electric motors using deep learning algorithms and its application: a review," *Energies*, vol. 14, no. 21, p. 7017, Oct. 2021, doi: 10.3390/en14217017.

[19] B. Jing, G. Liang, X. Dang, and Y. Jiang, "Reducing torque ripple for switched reluctance motors by current reshaping neural network," *Scientific Reports*, vol. 15, no. 1, p. 17530, May 2025, doi: 10.1038/s41598-025-02228-z.

[20] V. Lakshmi Devi, K. Kumar, S. R. Kiran, and N. M. Girish Kumar, "Analysis of energy management system in micro grid operations, load support, and control hierarchy," *2023 2nd International Conference on Trends in Electrical, Electronics and Computer Engineering, TEECCON 2023*, pp. 13–16, 2023, doi: 10.1109/TEECCON59234.2023.10335859.

[21] S. Krishnamoorthy and P. P. K. Panikkar, "Modified switching control of SRM drives for electric vehicles application with torque ripple reduction," *International Journal of Power Electronics and Drive Systems*, vol. 15, no. 1, pp. 147–159, 2024, doi: 10.11591/ijpeds.v15.i1.pp147-159.

[22] K. Kumar, N. R. Babu, and K. R. Prabhu, "Analysis of integrated Boost-Cuk high voltage gain DC-DC converter with RBFN MPPT for solar PV application," in *2017 Innovations in Power and Advanced Computing Technologies (i-PACT)*, IEEE, Apr. 2017, pp. 1–6. doi: 10.1109/IPACT.2017.8245072.

[23] J. L. Ba and D. P. Kingma, "Adam: A method for stochastic optimization," *3rd International Conference on Learning Representations, ICLR 2015 - Conference Track Proceedings*, pp. 1–15, 2015.

[24] S. Han, H. Mao, and W. J. Dally, "Deep compression: Compressing deep neural networks with pruning, trained quantization and Huffman coding," *4th International Conference on Learning Representations, ICLR 2016 - Conference Track Proceedings*, 2016.

[25] Z. Hou and Shangtai Jin, "Data-driven model-free adaptive control for a class of MIMO nonlinear discrete-time systems," *IEEE Transactions on Neural Networks*, vol. 22, no. 12, pp. 2173–2188, Dec. 2011, doi: 10.1109/TNN.2011.2176141.

[26] M. Benosman, "Model-based vs data-driven adaptive control: An overview," *International Journal of Adaptive Control and Signal Processing*, vol. 32, no. 5, pp. 753–776, May 2018, doi: 10.1002/acs.2862.

[27] H. Sarma and A. Bardalai, "An intelligent PID controller tuning for speed control of BLDC motor using driving training-based optimization," *International Journal of Power Electronics and Drive Systems*, vol. 14, no. 4, pp. 2474–2486, 2023, doi: 10.11591/ijpeds.v14.i4.pp2474-2486.

BIOGRAPHIES OF AUTHORS

S. Sudheer Kumar Reddy is a dedicated research scholar currently pursuing his Ph.D. at Sri Venkateshwara University College of Engineering, Tirupati. His academic foundation includes an M.Tech. degree from JNTU Anantapur and a B.Tech. from RGM Engineering College, Nandyal. With a robust teaching career spanning from 2013 to the present, he has contributed significantly as an educator in government polytechnics. Furthermore, he has played an instrumental role in his institution, serving as a member of various committees and actively participating in the successful attainment of NBA accreditation. He can be contacted at email: sudheersomu@gmail.com.

Dr. J. N. Chandra Sekhar is an associate professor in the Department of Electrical and Electronics Engineering, Sri Venkateswara University College of Engineering, Tirupati, India. He received his Ph.D. in Power Electronics and Drives from Sri Venkateswara University in 2019 and M.E. in Power Electronics and Industrial Drives from Sathyabama Institute of Science and Technology, Chennai, in 2006. His research interests include power electronics, electric drives, renewable energy systems, electric vehicles, and intelligent control techniques. He has published more than 30 papers in reputed SCI/Scopus-indexed journals and conferences, authored book chapters, and contributed to international publications. He also serves as an Academic Editor and reviewer for several leading journals and is a member of IEEE, ACM, and IEI. He can be contacted at email: chandu.jinka@gmail.com.